Charge transport and quantum phase transitions in singlet-superconductor/ferromagnet/singlet-superconductor junctions

Boris Kastening,[1,2] Dirk K. Morr,[3,4] Lambert Alff,[2] and Karl Bennemann[4]
[1]*Institut für Theoretische Physik, Technische Hochschule Aachen, Physikzentrum, 52056 Aachen, Germany*
[2]*Institut für Materialwissenschaft, Technische Universität Darmstadt, Petersenstraße 23, 64287 Darmstadt, Germany*
[3]*Department of Physics, University of Illinois at Chicago, Chicago, Illinois 60607, USA*
[4]*Institut für Theoretische Physik, Freie Universität Berlin, Arnimallee 14, 14195 Berlin, Germany*
(Received 11 November 2008; published 9 April 2009)

We study the Josephson current, I_J, in a junction consisting of two s-wave superconductors that are separated by a ferromagnetic barrier possessing magnetic and nonmagnetic scattering potentials, g and Z, respectively. We discuss the general dependence of I_J on g, Z, and the phase difference ϕ between the two superconductors. Moreover, we compute the critical current, I_c, for given g and Z, and show that it possesses two lines of nonanalyticity in the (g,Z) plane. We identify those regions in the (g,Z) plane where the Josephson current changes sign with increasing temperature without a change in the relative phase between the two superconductors, i.e., without a transition between the 0 and π states of the junction. Finally, we show that by changing the relative phase ϕ, it is possible to tune the junction through a first-order quantum phase transition in which the spin polarization of the two superconductors' combined ground state changes from $\langle S_z\rangle=0$ to $\langle S_z\rangle=1/2$.

DOI: 10.1103/PhysRevB.79.144508 PACS number(s): 74.50.+r, 74.45.+c, 74.78.−w, 85.25.Cp

I. INTRODUCTION

Heterostructures consisting of magnetically active layers provide new possibilities for manipulating charge (and potentially spin) transport and are hence of great interest for the field of spin electronics.[1] Josephson junctions consisting of conventional s-wave superconductors and a ferromagnetic barrier fall into this category, and their study has led to the discovery of a number of fundamentally new phenomena (for a recent review, see Ref. 2 and references therein). Among these is the transition from a 0 state to a π state in junctions with a metallic ferromagnetic barrier, which is accompanied by a sign change (and hence directional change) in the Josephson current. This transition signifies an intrinsic phase change of π between the superconductors forming the Josephson junction which arises from a temperature-dependent decay length and oscillation length of the superconducting order parameter inside the ferromagnetic metal. Such a transition was predicted theoretically[3] and subsequently also observed experimentally.[4] It was recently shown, by using a phenomenological S-matrix scattering formalism, that a sign change in the Josephson current with increasing temperature can also occur in insulating ferromagnetic barriers.[5,6] Changing the direction of the Josephson current by increasing temperature or by varying the relative phase between the superconductors leads to novel types of current switches that possess potential applications in quantum information technology.[1,7] Since most ferromagnetic barriers possess not only a magnetic scattering potential but also a nonmagnetic one, the question naturally arises to what extent the interplay between these two types of scattering potentials either alters the effects discussed above or leads to qualitatively new phenomena.

In this paper, we study the Josephson current, I_J, in a one-dimensional (1D) Josephson junction consisting of two s-wave superconductors and a thin (δ-function type) ferromagnetic barrier (SFS junction). We start from a microscopic Hamiltonian in which the barrier possesses magnetic and nonmagnetic scattering potentials, described by g and Z, respectively, with the former being directly proportional to the barrier magnetization. We discuss the general dependence of the charge Josephson current on g, Z, and the relative phase, ϕ, between the two superconductors. In particular, we demonstrate that in certain regions of the (g,Z) plane, I_J varies continuously with ϕ, while in other regions, and particularly around $Z=g$, I_J exhibits discontinuities. We compute the critical current, I_c, defined as the maximum Josephson current for a given g and Z, and we show that it possesses two lines of nonanalytic behavior in the (g,Z) plane. These nonanalyticities correspond to discontinuities in the first and second derivatives of I_c (with respect to g or Z). We show that I_c exhibits qualitatively different dependencies on the scattering strength in different parts of the (g,Z) plane, which opens the interesting (and quite counterintuitive) possibility to increase the critical current through the junction by increasing the junction magnetization. Moreover, we identify those regions of the (g,Z) plane in which the Josephson current changes sign (and thus direction) with increasing temperature without a change in the relative phase between the two superconductors, i.e., without a transition between the 0 and π states of the junction. In addition, we find that while the total spin Josephson current, I_s, flowing through the junction is zero, there are two contributions to I_s, arising from the Andreev and continuum states, respectively, that are equal in magnitude but possess opposite signs. We show that if these two contributions can be independently measured, this would open exciting venues for employing the combined spin and charge degrees of freedom in such a junction. Finally, we demonstrate that by changing the phase ϕ between the superconductors, it is possible to tune the junction through a first-order quantum phase transition in which the spin polarization of the two superconductors' combined ground state changes from $\langle S_z\rangle=0$ to $\langle S_z\rangle=1/2$. The theoretical methods used in this study provide direct insight into the explicit de-

pendence of the Josephson current and the Andreev states on the magnetization of the junction and into the interplay between magnetic and nonmagnetic scattering potentials.

II. THEORETICAL METHODS

We take the 1D SFS junction to be aligned along the z axis and to be described by the Hamiltonian

$$\mathcal{H} = \int dz \Bigg\{ \sum_{\sigma} \psi_{\sigma}^{\dagger}(z) \left[-\frac{\hbar^2 \partial_z^2}{2m} - \mu + U(z) \right] \psi_{\sigma}(z) - [\Delta(z)\psi_{\uparrow}^{\dagger}(z)\psi_{\downarrow}^{\dagger}(z) + \text{H.c.}] - \frac{g_e \mu_B \mu_0}{\hbar} \mathbf{M}(z) \cdot \sum_{\alpha,\beta} \psi_{\alpha}^{\dagger}(z) \vec{\boldsymbol{\sigma}}_{\alpha\beta} \psi_{\beta}(z) \Bigg\}, \tag{1}$$

where $\psi_{\sigma}^{\dagger}(z)$ and $\psi_{\sigma}(z)$ are the fermionic operators that create or annihilate a particle with spin σ at site z, respectively. $\Delta(z)$ is the s-wave superconducting gap, and $U(z)=U_0\delta(z)$ describes the nonmagnetic (i.e., potential) scattering strength of the junction at $z=0$. Without loss of generality, we choose the magnetization of the junction, $\mathbf{M}(z)$, to be parallel to the z axis, i.e., $\mathbf{M}(z)=M_0(0,0,1)\delta(z)$. In order to simplify the notation, we set $g_e\mu_B\mu_0/\hbar=1$. Moreover, to facilitate the discussion of the spin structure of the Josephson current and the junction ground state, we choose the quantization direction to coincide with the direction of the magnetic moment, i.e., with the z direction.

In the following, we use two complementary theoretical approaches in order to compute the Josephson current through the interface. One follows the Blonder-Tinkham-Klapwijk (BTK) approach[8] (see Sec. II A) and the other one starts from the quantum-mechanical definition of the current operator and computes its expectation value (see Sec. II B).

A. BTK ansatz

At the interface between the two superconductors, two Andreev bound states[9] with energies $E_{\alpha,\beta}$ are formed.[6,10] As was discussed before,[8,11,12] and as we will explicitly show in Sec. II B, the charge Josephson current flows solely through these two bound states and is hence given by[12]

$$I_J = I_J^{\alpha} + I_J^{\beta} = -\frac{e}{\hbar} \sum_{j=\alpha,\beta} \frac{\partial E_j}{\partial \phi} \tanh\left(\frac{E_j}{2k_B T} \right), \tag{2}$$

where ϕ is the phase difference between the superconducting order parameters on the left and right sides of the junction. In order to compute $E_{\alpha,\beta}$, we start from Eq. (1) and derive the Bogoliubov–de Gennes (BdG) equation[12–15] by introducing the unitary Bogoliubov transformation

$$\psi_{\uparrow}(z) = \sum_n u_{n,\alpha}(z)\alpha_n + v_{n,\beta}^*(z)\beta_n^{\dagger}, \tag{3a}$$

$$\psi_{\downarrow}(z) = \sum_n -u_{n,\beta}(z)\beta_n + v_{n,\alpha}^*(z)\alpha_n^{\dagger}, \tag{3b}$$

where the sum runs over all eigenstates of the junction and α_n, β_n are quasiparticle operators in terms of which the Hamiltonian, Eq. (1), is diagonal. Defining

$$\Psi_{n,j}(z) \equiv \begin{pmatrix} u_{n,j}(z) \\ v_{n,j}(z) \end{pmatrix} \tag{4}$$

with $j=\alpha,\beta$, the BdG equation is given by

$$\hat{H}_j \Psi_{n,j}(z) = E_{n,j} \Psi_{n,j}(z). \tag{5}$$

Here $E_{n,j}$ is the energy of the state $\Psi_{n,j}$,

$$\hat{H}_j = \begin{pmatrix} H_0 \mp H_M & -\Delta \\ -\Delta^* & -H_0 \mp H_M \end{pmatrix}, \tag{6}$$

where the upper (lower) sign corresponds to $j=\alpha(\beta)$ and

$$H_0 \equiv -\frac{\hbar^2 \partial_z^2}{2m} - \mu + U_0 \delta(z), \tag{7a}$$

$$H_M \equiv M_0 \delta(z), \tag{7b}$$

$$\Delta \equiv \begin{cases} \Delta_0 & z < 0 \\ \Delta_0 e^{-i\phi} & z > 0, \end{cases} \tag{7c}$$

with Δ_0 chosen real. The case $n=0$ corresponds to the Andreev bound states, and in what follows, we use E_j as a shorthand notation for their energies, $E_{0,j}$.

For the bound-state wave function on the left- and right-hand sides of the junction, $\Psi_{0,j,L}(z)$ and $\Psi_{0,j,R}(z)$, respectively, we make the ansatz

$$\Psi_{0,j,s}(z) = e^{c_s \kappa_j z} \sum_{\delta=\pm} \begin{pmatrix} u_{0,j,s,\delta} \\ v_{0,j,s,\delta} \end{pmatrix} e^{\delta i k_F z}, \tag{8}$$

with $s=L,R$, $c_{L,R}=\pm 1$, and k_F is the Fermi momentum. Note that the decay length of the Andreev state, $\kappa_j^{-1} = \hbar v_F / \sqrt{\Delta_0^2 - E_j^2}$ with $v_F=\hbar k_F/m$, itself depends on E_j. The solutions of Eq. (5) are subject to the boundary conditions

$$\Psi_{0,j,L}(0) = \Psi_{0,j,R}(0), \tag{9a}$$

$$\partial_z \Psi_{0,j,R}(0) - \partial_z \Psi_{0,j,L}(0) = \frac{2m}{\hbar^2} \begin{pmatrix} U_0 \mp M_0 & \\ & U_0 \pm M_0 \end{pmatrix} \times \Psi_{0,j,R}(0), \tag{9b}$$

where again the upper (lower) sign corresponds to $j=\alpha(\beta)$. In the limit $k_F \gg \kappa_j$, which holds for superconductors with coherence length $\xi_c = v_F/\Delta_0 \gg 1/k_F$, the solution of the BdG equation yields two Andreev states with energies

$$\frac{E_j}{\Delta_0} = \frac{\sqrt{A+B} \mp \sqrt{A-B}}{\sqrt{2[1+(g+Z)^2][1+(g-Z)^2]}}, \tag{10}$$

where the upper (lower) sign corresponds to $j=\alpha(\beta)$ and

$$A = (1+Z^2-g^2)[\cos^2(\phi/2) + Z^2 - g^2] + 2g^2, \tag{11a}$$

$$B = \sqrt{[1+(g+Z)^2][1+(g-Z)^2][\cos^2(\phi/2) + Z^2 - g^2]}, \tag{11b}$$

with $g=mM_0/\hbar^2 k_F$ and $Z=mU_0/\hbar^2 k_F$. Without loss of generality we assume $g, Z \geq 0$ from here on. While E_{β} does not change sign as a function of ϕ (for $Z \neq 0$), E_{α} changes sign if

$0<g^2-Z^2<1$ (hence for $g\leq Z$ or $g\geq\sqrt{1+Z^2}$, no sign change in either bound state takes place). This sign change, which occurs at a phase difference ϕ_c^α given by $\cos^2(\phi_c^\alpha/2)=g^2-Z^2$, indicates a first-order phase transition in which the spin polarization of the superconductors' ground state changes, as discussed in more detail in Sec. III C.

For the subsequent discussion, it is necessary to consider the spin structure of the Andreev states. To this end, we compute the local density of states (LDOS), $N(\sigma,z)$ (i.e., the local spectral function), for the spin-↑ and spin-↓ components of the Andreev states, which, using the Bogoliubov transformation presented in Eq. (3), are readily obtained as

$$N(\uparrow,z)=|u_{0,\alpha}(z)|^2\delta(\omega-E_\alpha)+|v_{0,\beta}(z)|^2\delta(\omega+E_\beta), \tag{12a}$$

$$N(\downarrow,z)=|u_{0,\beta}(z)|^2\delta(\omega-E_\beta)+|v_{0,\alpha}(z)|^2\delta(\omega+E_\alpha). \tag{12b}$$

Hence (for $E_{\alpha(\beta)}>0$), the wave function of the α state, $|\Psi_{0,\alpha}\rangle$, possesses a particlelike spin-↓ component, and a holelike spin-↑ component, i.e., $|\Psi_{0,\alpha}\rangle=|p,\downarrow\rangle+|h,\uparrow\rangle$. Similarly for the β state, $|\Psi_{0,\beta}\rangle=|p,\uparrow\rangle+|h,\downarrow\rangle$. When E_α changes sign, the occupation numbers of the spin-↑ and spin-↓ components of the respective wave function are interchanged. We thus find that the LDOS near the junction barrier contains four peaks inside the superconducting gap, in agreement with the results obtained in Refs. 6 and 10. As an important check of our calculations, we consider the limit $\phi=0$, where the Josephson junction is identical to a system, in which a single magnetic impurity is located inside a 1D s-wave superconductor. In this limit, Eq. (10) yields that only one of the Andreev states exists inside the superconducting gap with $E_\alpha<\Delta_0$, while the other Andreev state possesses the energy $E_\beta=\Delta_0$ and is thus part of the continuum [see Fig. 1(a)]. These results are in agreement with those of the $\hat{T}$-matrix and Bogoliubov–de Gennes approaches used in the context of impurity scattering in s-wave superconductors (for a recent review, see Ref. 16). We note that in this limit, $\phi=0$, our results (and those of Ref. 16) for $E_{\alpha,\beta}$ do not agree with the findings in Refs. 5 and 6 (see also Ref. 17).

B. Quantum-mechanical current

Using the operator definition of the quantum-mechanical current, we may resolve the spin-↑ and spin-↓ particle currents $I_\uparrow(z)$ and $I_\downarrow(z)$, which in turn allows to compute the charge and spin currents via

$$I_J(z)\equiv -e[I_\uparrow(z)+I_\downarrow(z)], \tag{13a}$$

$$I_S(z)\equiv\frac{\hbar}{2}[I_\uparrow(z)-I_\downarrow(z)]. \tag{13b}$$

In order to obtain appropriately defined current operators $\hat{I}_\uparrow(z)$ and $\hat{I}_\downarrow(z)$, whose expectation values are the currents $I_\uparrow(z)$ and $I_\downarrow(z)$, we note that the density operator of spin-σ electrons is

$$\hat{\rho}_\sigma(z)=\hat{\rho}_\sigma(z,z')|_{z'=z}, \tag{14}$$

where

$$\hat{\rho}_\sigma(z,z')\equiv\psi_\sigma^\dagger(z)\psi_\sigma(z'). \tag{15}$$

The quantum-mechanical particle current operator corresponding to $\hat{\rho}_\sigma(z)$ then follows from

$$\hat{I}_\sigma(z)=\frac{i\hbar}{2m}[(\partial_z-\partial_{z'})\hat{\rho}_\sigma(z,z')]|_{z'=z}$$

$$=\frac{i\hbar}{2m}\{[\partial_z\psi_\sigma^\dagger(z)]\psi_\sigma(z)-\psi_\sigma^\dagger(z)[\partial_z\psi_\sigma(z)]\}, \tag{16}$$

and its expectation value

$$I_\sigma(z)=\frac{\hbar}{m}\mathrm{Im}\langle\psi_\sigma^\dagger(z)[\partial_z\psi_\sigma(z)]\rangle \tag{17}$$

is the corresponding particle current. In what follows, we refer to $I_\sigma(z)$ as the "conventional" form of the particle current.

After diagonalizing the Hamiltonian with the Bogoliubov transformation of Eq. (3), the currents given in Eq. (13) possess in general contributions from both the Andreev bound states and the continuum states. The calculation of the latter is prohibitively cumbersome when using the form of I_σ given in Eq. (17). It turns out, however, that one can use an alternative formulation to evaluate I_σ by defining a "symmetrized" form of the current operator. Specifically, using the anticommutator

$$\{\psi_\sigma^\dagger(z),\psi_{\sigma'}(z')\}=\delta_{\sigma\sigma'}\delta(z-z'), \tag{18}$$

we can write

$$\hat{\rho}_\sigma(z,z')\equiv\frac{1}{2}[\delta(z-z')+\psi_\sigma^\dagger(z)\psi_\sigma(z')-\psi_\sigma(z')\psi_\sigma^\dagger(z)]. \tag{19}$$

We next define a symmetrized density via

$$\hat{\rho}_\sigma^{\mathrm{sym}}(z,z')\equiv\frac{1}{2}[\psi_\sigma^\dagger(z)\psi_\sigma(z')+\psi_\sigma(z)\psi_\sigma^\dagger(z')], \tag{20}$$

where the second term on the right-hand side of Eq. (20) arises from the first term via a particle-hole transformation [this fact becomes important when discussing the form of the LDOS corresponding to $\hat{\rho}_\sigma^{\mathrm{sym}}(z,z)$, see below]. Since the δ-function in Eq. (19) does not contribute to the particle current operator, it immediately follows that the densities defined in Eqs. (19) and (20) when inserted into Eq. (16) yield the same spin-σ particle current operator. We can therefore write $\hat{I}_\sigma$ in a symmetrized form as

$$\hat{I}_\sigma(z)=\frac{i\hbar}{2m}[(\partial_z-\partial_{z'})\hat{\rho}_\sigma^{\mathrm{sym}}(z,z')]|_{z'=z}$$

$$=-\frac{i\hbar}{4m}\{\psi_\sigma^\dagger(z)[\partial_z\psi_\sigma(z)]+\psi_\sigma(z)[\partial_z\psi_\sigma^\dagger(z)]-\mathrm{H.c.}\}. \tag{21}$$

One then obtains

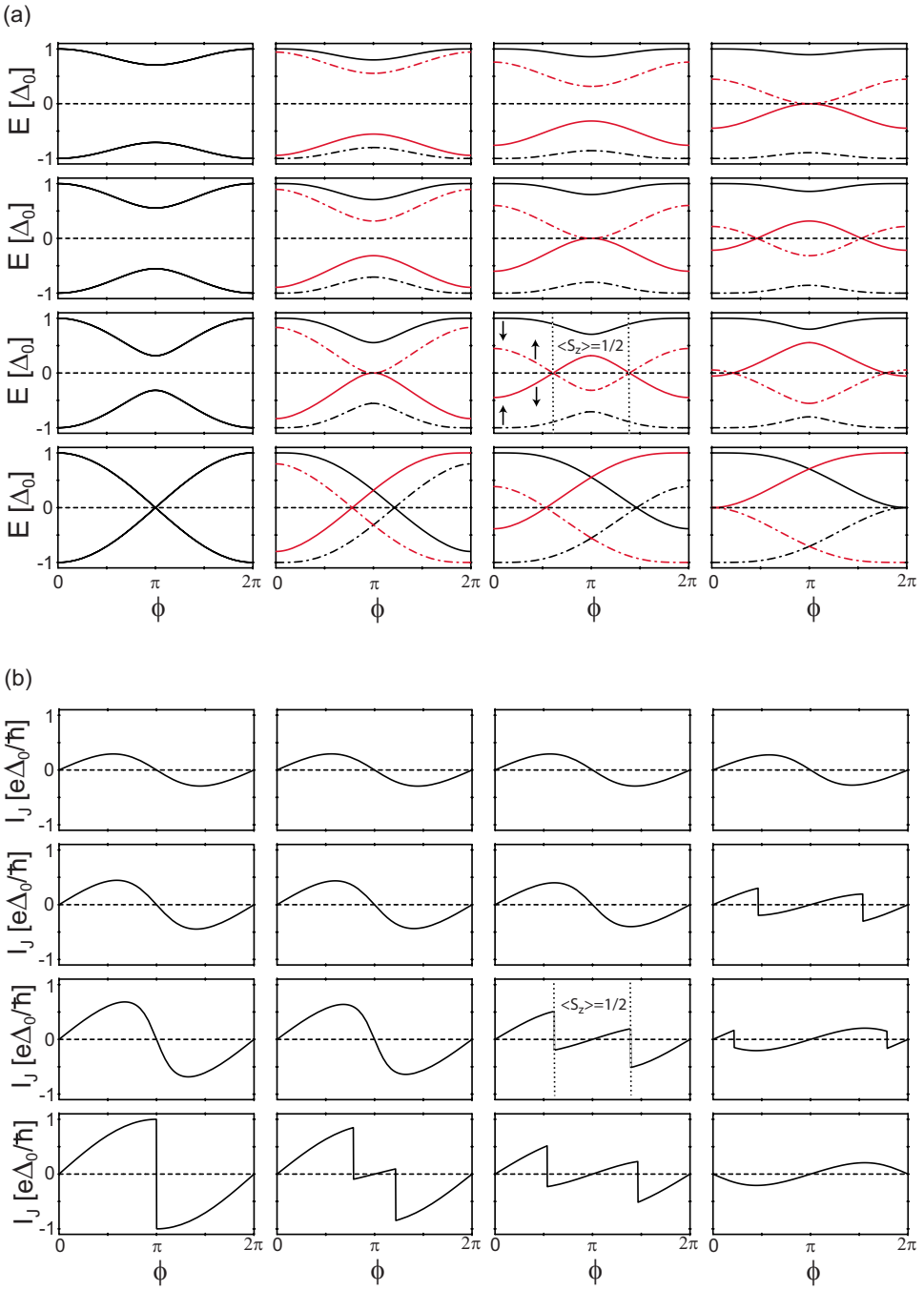

FIG. 1. (Color online) (a) Energies $\pm E_{\alpha,\beta}$ of the Andreev states. The columns from left to right correspond to $g=0,\frac{1}{3},\frac{2}{3},1$, respectively, while the rows from bottom to top correspond to $Z=0,\frac{1}{3},\frac{2}{3},1$, respectively. The energies of the α and β states are indicated by red (gray in print) and black lines, respectively, while the spin-$\uparrow$ and spin-$\downarrow$ components are indicated by dashed-dotted and solid lines. For $g=0$ (left column) the α and β states are degenerate. (b) The resulting I_J at $T=0$ for several g and Z as a function of ϕ.

$$I_\sigma(z) = \frac{\hbar}{2m}\mathrm{Im}\langle \psi_\sigma^\dagger(z)\partial_z\psi_\sigma(z) + \psi_\sigma(z)\partial_z\psi_\sigma^\dagger(z)\rangle \qquad (22)$$

as the corresponding symmetrized form of the spin-σ particle current. While the current thus defined is identical to the conventional form given in Eq. (17), it turns out that the calculation of the contributions from continuum states using the right-hand side of Eq. (22) is considerably simplified. In what follows, we therefore discuss the contributions of continuum and Andreev states to the charge and spin current using the symmetrized form of the particle current, Eq. (22).

Since the contributions to the particle current arising from individual (Andreev or continuum) states are different in the conventional and the symmetrized forms, we distinguish between them by denoting with (without) a tilde the current flowing through a specific state within the symmetrized (conventional) definition. We then obtain

$$I_{\uparrow(\downarrow)}(z) = \sum_n \tilde{I}_{\uparrow(\downarrow),n}(z), \qquad (23)$$

where

$$\tilde{I}_{\uparrow,n}(z) \equiv I^u_{n,\alpha}(z)\tanh\frac{\beta E_{n,\alpha}}{2} + I^v_{n,\beta}(z)\tanh\frac{\beta E_{n,\beta}}{2}, \quad (24a)$$

$$\tilde{I}_{\downarrow,n}(z) \equiv I^u_{n,\beta}(z)\tanh\frac{\beta E_{n,\beta}}{2} + I^v_{n,\alpha}(z)\tanh\frac{\beta E_{n,\alpha}}{2}, \quad (24b)$$

with amplitude functions

$$I^f_{n,j}(z) \equiv \frac{\hbar}{2m}\mathrm{Im}[f_{n,j}(z)\partial_z f^*_{n,j}(z)], \quad (25)$$

where $f=u,v$ and $j=\alpha,\beta$, and the sum in Eq. (23) runs over all states of the system (including Andreev and continuum states).

We begin by computing the contribution to the total current arising from the continuum states. Using the general ansatz for the form of these states described in Appendix A, we find that the continuum states with momentum $\pm(k_F \pm q)$ are degenerate and that their energy E_q is given by (in the limit $E_q \ll \mu$)

$$E_q^2 = |\Delta_0|^2 + \left(\frac{\hbar^2 k_F q}{m}\right)^2. \quad (26)$$

Diagonalizing the corresponding subspace, one obtains three important relations,

$$\sum_{n(E_q)} [\tilde{I}_{\uparrow,n}(z) + \tilde{I}_{\downarrow,n}(z)] \propto \sin 2q|z|, \quad (27a)$$

$$\sum_{n(E_q)} [\tilde{I}_{\uparrow,n}(z) - \tilde{I}_{\downarrow,n}(z)] = 0, \quad (27b)$$

$$\sum_{n(E_q)} I^u_{n,\alpha(\beta)}(z=0) = \sum_{n(E_q)} I^v_{n,\alpha(\beta)}(z=0), \quad (27c)$$

where the sums run over an orthonormal basis of continuum states with energy E_q. The first relation, Eq. (27a), implies that given the definition of the charge Josephson current, I_J, in Eq. (13a), the contribution to I_J from the continuum states at the interface is identically zero within the symmetrized version of the current. As we show below, this result also holds when the conventional definition of the current operator is used. General arguments have been put forward that this result arises since the density of continuum states in the presence of a barrier is unchanged.[18] However, away from the interface the continuum states carry a nonzero charge current since charge conservation requires that the (decaying) current through the Andreev states be compensated by a current carried through the continuum states. The second relation, Eq. (27b), implies that the contribution of the continuum states to the spin Josephson current, as defined in Eq. (13b), is zero at any position z along the junction. Finally, the third relation, Eq. (27c), when combined with Eq. (24), yields that at the barrier, there are no contributions from the continuum states to either the spin-$\uparrow$ or spin-$\downarrow$ particle current.

Since the continuum states carry no charge current at the barrier (i.e., at $z=0$), the total charge Josephson current is solely carried by the Andreev states and thus given by

$$I_J \equiv I_J(0) = -e[\tilde{I}^{\mathrm{AS}}_{\uparrow}(0) + \tilde{I}^{\mathrm{AS}}_{\downarrow}(0)], \quad (28)$$

where $\tilde{I}^{\mathrm{AS}}_{\uparrow,\downarrow}$ are the currents through the Andreev states in the symmetric formulation of the current. These are given by the $n=0$ term in Eq. (23) for which one thus has

$$\tilde{I}^{\mathrm{AS}}_{\uparrow}(z) = I^u_{0,\alpha}(z)\tanh\frac{\beta E_\alpha}{2} + I^v_{0,\beta}(z)\tanh\frac{\beta E_\beta}{2}, \quad (29a)$$

$$\tilde{I}^{\mathrm{AS}}_{\downarrow}(z) = I^u_{0,\beta}(z)\tanh\frac{\beta E_\beta}{2} + I^v_{0,\alpha}(z)\tanh\frac{\beta E_\alpha}{2}. \quad (29b)$$

It is straightforward to show that the bound-state ansatz of Eq. (8) leads to

$$I^u_{0,\alpha}(z) = I^v_{0,\alpha}(z) \propto e^{-2\kappa|z|}, \quad (30a)$$

$$I^u_{0,\beta}(z) = I^v_{0,\beta}(z) \propto e^{-2\kappa|z|}, \quad (30b)$$

yielding $\tilde{I}^{\mathrm{AS}}_{\uparrow}(z) = \tilde{I}^{\mathrm{AS}}_{\downarrow}(z)$. Together with Eq. (27b), this result implies that within the symmetrized form of the particle current, Eq. (22), neither the continuum states nor the Andreev bound states carry a spin current. Hence, we obtain that the total spin current $I_S(z)$ defined in Eq. (13b) vanishes at any point along the junction, in agreement with the arguments in Ref. 19. This result holds even when the system undergoes a first-order quantum phase transition in which the spin polarization of the junction ground state changes (see Sec. III C).

While the symmetrized form of the Josephson current used above allowed for a simpler evaluation of the contributions arising from the continuum states, any physical interpretation of the Josephson current has to be based on its conventional definition, given by Eq. (16), and the form of the spin density in Eq. (15). In what follows, we therefore discuss the form of the charge and spin currents within the conventional definition and compare them with the symmetrized results presented above. A connection between the expressions for $\tilde{I}_{\sigma,n}$ and $I_{\sigma,n}$ (which represent the currents flowing through state n in the symmetrized and conventional definition, respectively) can be made by using the following identities:

$$\sum_n [I^u_{n,\alpha}(z) - I^v_{n,\beta}(z)] = 0, \quad (31a)$$

$$\sum_n [I^u_{n,\beta}(z) - I^v_{n,\alpha}(z)] = 0, \quad (31b)$$

where, as in Eq. (23), the sum runs over all states of the junction. These identities are derived by applying $\partial_z - \partial_{z'}$ to the anticommutator in Eq. (18), and subsequently setting $\sigma' = \sigma$ and $z' = z$, and using the form of $\psi_\uparrow(z)$ and $\psi_\downarrow(z)$ given in Eq. (3). One then finds that by subtracting the left-hand side of Eq. (31a) [Eq. (31b)] from the right-hand side of Eq. (23) for $\sigma=\uparrow$ [$\sigma=\downarrow$], one obtains the corresponding expressions for $I_{\sigma,n}$. In particular, within the conventional definition, the Josephson current through the Andreev bound states is given by

$$I_{\uparrow}^{\mathrm{AS}}(z) = -I_{0,\alpha}^{u}(z)\left(1-\tanh\frac{\beta E_{\alpha}}{2}\right)+I_{0,\beta}^{v}(z)\left(1+\tanh\frac{\beta E_{\beta}}{2}\right), \tag{32a}$$

$$I_{\downarrow}^{\mathrm{AS}}(z) = -I_{0,\beta}^{u}(z)\left(1-\tanh\frac{\beta E_{\beta}}{2}\right)+I_{0,\alpha}^{v}(z)\left(1+\tanh\frac{\beta E_{\alpha}}{2}\right). \tag{32b}$$

Given the result for I_J in Eq. (28), it immediately follows that

$$I_J = -e[I_{\uparrow}^{\mathrm{AS}}(0)+I_{\downarrow}^{\mathrm{AS}}(0)], \tag{33}$$

implying that also within the conventional definition of the particle current, the total charge Josephson current at $z=0$ is solely carried by the Andreev states with no contribution arising from the continuum states. This result justifies the use of Eq. (2) in the BTK approach of Sec. II A for the calculation of the total charge Josephson current. Moreover, since the charge Josephson currents computed within the BdG approach of Sec. II A should be the same as that of the quantum-mechanical method of Sec. II B, one requires [by combining Eqs. (2), (28), (29a), (29b), (30a), and (30b)] that the following important identity be satisfied:

$$\frac{\partial E_j}{\partial \phi} = 2\hbar I_{0j}^{v}(0), \tag{34}$$

with $j=\alpha,\beta$. We have carried out an extensive numerical survey in the parameter space of our system and found this relation to always hold.

We next consider the form of the spin current in the conventional definition of the currents. While the result of a vanishing total spin current, which we obtained within the symmetrized form, also has to hold within the conventional framework, we find that the contributions from the Andreev and continuum states differ. In particular, using the results of Eq. (32), we find that the contribution of the Andreev states to the spin current, I_S^{AS}, is given by

$$I_S^{\mathrm{AS}}(z) = \hbar[I_{0,\beta}^{v}(z)-I_{0,\alpha}^{v}(z)], \tag{35}$$

which in general does not vanish. However, since the total spin current still needs to be zero, it immediately follows that within the conventional definition of the particle current, a spin current of equal magnitude but opposite sign to I_S^{AS} flows through the continuum states. Note, however, that while a spin Josephson current flows through the continuum states, the charge current through these states is zero, as discussed above. The contribution to the spin current provided by the continuum states thus compensates the spin current through the Andreev states and leads to a zero total spin current [we return to a discussion of these two (opposite) contributions to the spin current in Sec. III B]. In contrast, in the symmetrized version, the spin currents through the continuum states on one hand, and the Andreev states on the other hand, are exactly zero.

In order to understand the different origin of the zero-spin current in these two frameworks and to gain insight into its physically correct interpretation, we consider the local density of states of the Andreev states, $N^{\mathrm{sym}}(\sigma,z)$, corresponding to the density $\rho_{\sigma}^{\mathrm{sym}}(z)=\langle\hat{\rho}_{\sigma}^{\mathrm{sym}}(z,z)\rangle$, which is given by

$$N^{\mathrm{sym}}(\uparrow,z) = \frac{1}{2}|u_{0,\alpha}(z)|^2[\delta(\omega-E_{\alpha})+\delta(\omega+E_{\alpha})] + \frac{1}{2}|v_{0,\beta}(z)|^2[\delta(\omega+E_{\beta})+\delta(\omega-E_{\beta})], \tag{36a}$$

$$N^{\mathrm{sym}}(\downarrow,z) = \frac{1}{2}|u_{0,\beta}(z)|^2[\delta(\omega-E_{\beta})+\delta(\omega+E_{\beta})] + \frac{1}{2}|v_{0,\alpha}(z)|^2[\delta(\omega+E_{\alpha})+\delta(\omega-E_{\alpha})]. \tag{36b}$$

Here, the second term on the right-hand side of each equation is obtained from the first one via a particle-hole transformation, in agreement with the definition of $\hat{\rho}_{\sigma}^{\mathrm{sym}}(z,z')$ in Eq. (20). As a result, the system now possesses two sets of two degenerate bound states, i.e., a total of four Andreev bound states, each with a spectral weight of 1/2. Within each set, the degenerate bound states differ by their spin quantum number: one bound state possesses a particle (hole) branch which is spin $\uparrow$ (spin $\downarrow$) and vice versa for the second bound state. Using the relations in Eqs. (30) and (34) and the definition of the Josephson current in Eqs. (2) and (13a), one immediately finds that such a LDOS leads to the expressions for $\tilde{I}_{\uparrow,\downarrow}^{\mathrm{AS}}(z)$ given in Eq. (29). Since the spin quantum numbers are opposite between the degenerate bound states, it naturally follows that the spin current through the Andreev states is zero. Note, however, that the LDOS given in Eq. (36) is unphysical; it does not reflect the symmetry breaking of the ferromagnetic barrier since for every spin-$\uparrow$ branch, there exists a degenerate spin-$\downarrow$ branch. Moreover, in the limit $\phi=0$ (where the barrier represents a single magnetic impurity in a 1D s-wave superconductor), the symmetrized LDOS of Eq. (36) is in disagreement with that obtained from the $\hat{T}$-matrix and Bogoliubov–de Gennes approaches.[16] In contrast, the LDOS of Eq. (12) which is based on the conventional definition of the density operator reflects the symmetry breaking of the ferromagnetic barrier. It is therefore physical and in full agreement with the results of Ref. 16 for $\phi=0$. It then follows that the physically correct interpretation regarding the origin of a zero total spin current is that both the Andreev states and the continuum states carry a spin current of equal magnitude but opposite sign. We propose that this conclusion can be tested by using a spin-resolved scanning tunneling microscopy (STM) experiment which can distinguish between the LDOS presented in Eq. (12) on one hand and that given in Eqs. (36) on the other hand.

III. RESULTS

A. Charge transport

The general dependence of the Andreev state energies and the Josephson current on the scattering strength of the barrier

is presented in Fig. 1 where we plot $\pm E_{\alpha,\beta}$ [Fig. 1(a)] and the resulting Josephson current at $T=0$ [Fig. 1(b)] as a function of ϕ for several values of Z and g [the columns in Figs. 1(a) and 1(b) from left to right correspond to $g=0,\frac{1}{3},\frac{2}{3},1$, respectively, while the rows from bottom to top correspond to $Z=0,\frac{1}{3},\frac{2}{3},1$, respectively]. For a purely nonmagnetic barrier [i.e., $g=0$, left column of Fig. 1(a)], we find in agreement with earlier results[6,12–14,20] that the Andreev states are degenerate with energies,

$$\frac{E_{\alpha,\beta}}{\Delta_0} = \sqrt{\frac{\cos^2(\phi/2)+Z^2}{1+Z^2}}. \tag{37}$$

This degeneracy is lifted by a nonzero magnetic scattering potential of the junction (i.e., $g\neq 0$) as shown in the three right columns of Fig. 1(a). A qualitatively similar result was also found in Refs. 6, 10, 17, and 19. Specifically, for a purely magnetic scattering potential of the junction [i.e., $Z=0$, bottom row of Fig. 1(a)], the energies of the Andreev states are given by

$$\frac{E_{\alpha,\beta}}{\Delta_0} = \frac{1}{1+g^2}[\cos(\phi/2) \mp g\sqrt{g^2+\sin^2(\phi/2)}]. \tag{38}$$

In agreement with the analytical results presented in Eqs. (37) and (38) we find that with increasing $g \gg Z$ [plots in the lower-right corner of Fig. 1(a)] and $Z \gg g$ [plots in the upper-left corner of Fig. 1(a)], the energies of both bound states move toward the gap edge. An interesting situation occurs for $g=Z$ [plots along the diagonal of Fig. 1(a)], since in this case, the effective scattering strength for the spin-$\downarrow$ and spin-$\uparrow$ electrons is $V_{\mathrm{eff}}^{\downarrow}=g+Z=2Z$ and $V_{\mathrm{eff}}^{\uparrow}=g-Z=0$, respectively. In the unitary scattering limit $g=Z\gg 1$, we then find that the energies of the Andreev states are given by

$$\frac{E_\alpha}{\Delta_0} = \frac{\cos^2(\phi/2)}{2Z} + \mathcal{O}(Z^{-3}), \tag{39a}$$

$$\frac{E_\beta}{\Delta_0} = 1 - \frac{\sin^4(\phi/2)}{8Z^2} + \mathcal{O}(Z^{-4}). \tag{39b}$$

Hence, in the limit $g=Z\to\infty$, the α state becomes a zero-energy (midgap) state, while the β state moves into the continuum. This analytical result is confirmed by the numerical results shown in the plots along the diagonal of Fig. 1(a).

We next discuss the form of the Josephson current, resulting from the form of the Andreev states shown in Fig. 1(a). In the unitary scattering limit $Z \gg \max\{g,1\}$ the Josephson current at $T=0$ is given by (to leading order in Z)

$$I_J = \frac{e\Delta_0}{\hbar}\frac{\sin\phi}{2Z^2}, \tag{40}$$

while for $g \gg \max\{Z,1\}$ one obtains to leading order in g,

$$I_J = -\frac{e\Delta_0}{\hbar}\frac{\sin\phi}{2g^2}. \tag{41}$$

Hence, the Josephson currents for a predominantly nonmagnetic [Eq. (40)] and predominantly magnetic [Eq. (41)] barrier differ by a phase shift of π in the unitary scattering limit. This result also follows from a comparison of the I_J plots in the upper-left ($Z \gg g$) and lower-right ($g \gg Z$) corners of Fig. 1(b).

Whether the Josephson current in the junction considered here is carried by Cooper pairs, or by single electrons, depends on the relative strength of g and Z. We first recall that in a purely nonmagnetic junction (i.e., $g=0$), it was argued that the dependence of the Josephson current on Z in the unitary scattering limit, $I_J \sim Z^{-2}$ [see Eq. (40)], implies that the current is carried by Cooper pairs.[13,14] In contrast, in Josephson junctions consisting of unconventional superconductors, the scaling of the Josephson current, $I_J \sim Z^{-1}$, implies that it is carried by single electrons.[14] Here, we find that for a predominantly magnetic junction with $g \gg \max\{Z,1\}$, I_J also scales with the inverse square of the scattering strength [see Eq. (41)] and the current should thus also be carried by Cooper pairs. In contrast, for the case $Z=g\to\infty$, we obtain $I_J \sim Z^{-1}$ and the Josephson current should thus be carried by single electrons. Further support for this conclusion comes from considering the dependence of E_α on the scattering strength in the limit $\phi=0$. As mentioned above, in this case, the junction is identical to a static impurity in a (1D) s-wave superconductor.[21] If the impurity is purely magnetic, the Andreev state α (which is better known in this context as a Shiba state) is formed through scattering processes involving the creation and destruction of Cooper pairs. This immediately follows from a diagrammatic derivation of the scattering $\hat{T}$ matrix which includes diagrams that contain the anomalous Green's functions, F and F^*, representing the creation and destruction of Cooper pairs, respectively.[21] As a direct result of the included anomalous Green's functions, one obtains $E_\alpha \sim g^{-2}$, as in Eq. (38) which immediately leads to $I_J \sim g^{-2}$ for $\phi \neq 0$. In contrast, for an impurity with scattering strength $V_{\mathrm{eff}}^{\downarrow}=2Z$ and $V_{\mathrm{eff}}^{\uparrow}=0$, the $\hat{T}$ matrix is given by a series of diagrams that contain the normal Green's function only (diagrams containing F and F^* are forbidden), and hence $E_\alpha \sim Z^{-1}$. Note that for the same reason, Josephson junctions consisting of unconventional superconductors possess Andreev states whose energies also scale as $E_i \sim Z^{-1}$. This connection between the scaling of E_α and I_J for $\phi \neq 0$ with the case of impurity scattering for $\phi=0$ demonstrates that the presence or absence of scattering diagrams involving the anomalous Green's function determines the nature of the Josephson current.

While the Josephson current is a continuous function of ϕ for certain combinations of Z and g, I_J also exhibits discontinuities, in particular, in the vicinity of $Z \approx g$, as shown in Fig. 1(b). These discontinuities arise from a zero-energy crossing of an Andreev state at a certain phase, ϕ_{LC}, where $\partial E_{\alpha,\beta}/\partial\phi \neq 0$, as shown in Fig. 1(a). Since at $T=0$, only the negative-energy branches of the bound states are populated and thus contribute to I_J, $\partial E_{\alpha,\beta}/\partial\phi \neq 0$ leads to a discontinuity in the Josephson current at ϕ_{LC}. In Fig. 2(a), we present a contour plot that represents in which parts of the (g,Z) plane I_J exhibits a continuous or discontinuous dependence on ϕ. In the white regions of Fig. 2(a), I_J is continuous, while in the gray and black regions, which are located in the vicinity of the $Z=g$ line, it exhibits discontinuities as ϕ is varied.

This change between continuous and discontinuous behaviors of I_J in the (g,Z) plane leads to an interesting form

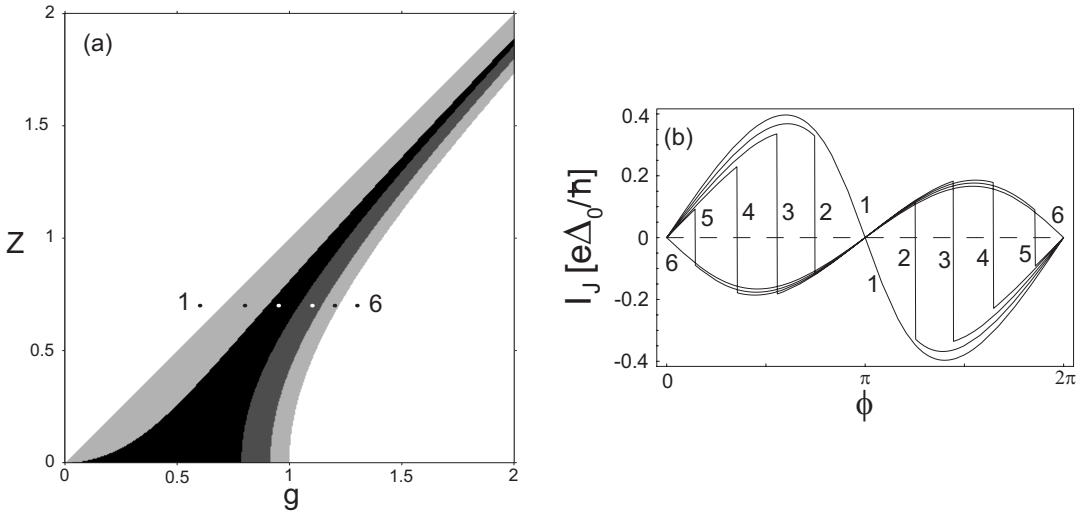

FIG. 2. (a) Behavior of $I_J(\phi)$ in the (g,Z) plane. White regions: I_J is continuous. Light (dark) gray regions: maximum of $|I_J(\phi)|$ is realized at a continuous extremum (discontinuity). Black area: only extrema at discontinuities exist. The white regions are bounded by $Z^2=g^2$ and by $Z^2=g^2-1$. (b) $I_J(\phi)$ at $T=0$ for the six parameter pairs (g,Z) indicated by dots in (a).

of the critical current, I_c. Here, we define I_c for a given g and Z as the maximum absolute value of I_J for any $0\leq\phi<\pi$, i.e., $I_c=\max_\phi[|I_J(\phi)|]$. At that value of ϕ, for which $|I_J(\phi)|$ exhibits the maximum value, I_J possesses either a continuous extremum or a discontinuity. In the light (dark) gray areas of Fig. 2(a), I_c is realized at a continuous extremum (discontinuity), while the discontinuity (continuous extremum) realizes a local maximum of $|I_J|$ only. In the black regions of Fig. 2(a), no continuous extremum exists. In order to investigate the origin of the qualitatively different behavior of I_J in the white, gray, and dark regions, we consider six pairs of values (g,Z), denoted by the dots in Fig. 2(a), and present the resulting Josephson currents as a function of ϕ in Fig. 2(b). We find that the different behavior in the gray and black regions arises from a shift in the values of ϕ at which the discontinuity in I_J occurs. As one moves from points (1) to (6) in Fig. 2 two discontinuities first emerge at $\phi=\pi$ and then move symmetrically toward $\phi=0$ and $\phi=2\pi$, respectively.

In Fig. 3(a), we present a contour plot of the critical current in the (g,Z) plane, with the white (dark gray) areas indicating a large (small) critical current. An analytical expression for the critical current in the (g,Z) plane can be obtained along the lines $g=0$ and for $Z=0$, where one finds

$$I_c(g=0,Z)=\frac{e\Delta_0}{\hbar}\left(1-\frac{Z}{\sqrt{1+Z^2}}\right), \tag{42}$$

$$I_c(g,Z=0)=\begin{cases}\dfrac{e\Delta_0}{\hbar}\dfrac{\sqrt{1-g^2}}{1+g^2} & 0\leq g\leq g_m\\ \dfrac{e\Delta_0}{\hbar}\left(\dfrac{g}{\sqrt{1+g^2}}-\dfrac{g^2}{1+g^2}\right) & g\geq g_m,\end{cases} \tag{43}$$

where $g_m\approx 0.915\,186$ is the largest real solution of the equation $4g^6-4g^2+1=0$.

Even though the critical current is a continuous function of g and Z, it possesses two lines of nonanalyticity in the (g,Z) plane that asymptotically approach $Z=g$ for $Z,g\to\infty$. These lines are represented in Fig. 3(a) as solid black lines. Line (1), corresponding to the boundary between the light gray and black regions in Fig. 2(a), represents a discontinuity in the second derivative of I_c. In contrast, line (2), which corresponds to the boundary between the light gray and dark gray regions in Fig. 2(a), represents a discontinuity in the first derivative of I_c. Line (2) also represents a sign change in that value of I_J which determines I_c. In other words, to the left (right) of line (2), I_c is realized by a positive (negative) value of I_J. These nonanalyticities become particularly apparent when one plots the critical current as a function of g (for constant Z) and Z (for constant g), as shown in Figs. 3(b) and 3(c), respectively [in Fig. 3(b), we indicated the nonanalyticities for the curve with $Z=1/2$ by arrows].

The different dependence of I_J on the scattering strength in the limits $g\gg Z$ or $Z\gg g$ [see Eqs. (40) and (41)] on one hand and $g=Z\gg 1$, where

$$I_J^\alpha=\frac{e\Delta_0}{\hbar}\frac{\sin\phi}{4Z}, \tag{44a}$$

$$I_J^\beta=\frac{e\Delta_0}{\hbar}\frac{\sin\phi(1-\cos\phi)}{16Z^2}, \tag{44b}$$

on the other hand leads to the interesting possibility to increase the critical current by increasing the magnetization, and hence the scattering strength of the barrier. Specifically, we find $I_c=\frac{e\Delta_0}{2\hbar}g^{-2}$ for $g\gg Z$ and $I_c=\frac{e\Delta_0}{2\hbar}Z^{-2}$ for $Z\gg g$, while for $Z=g\gg 1$, we have $I_c=\frac{e\Delta_0}{4\hbar}Z^{-1}$. As a result, we find that for fixed $Z\gg 1$ and increasing g, the critical current exhibits a maximum at $Z=g$. This effect is demonstrated in Fig. 4 where we present I_c as a function of g for $Z=20$. Hence, for a given nonmagnetic scattering strength of a paramagnetic barrier, it is possible to increase the critical current by in-

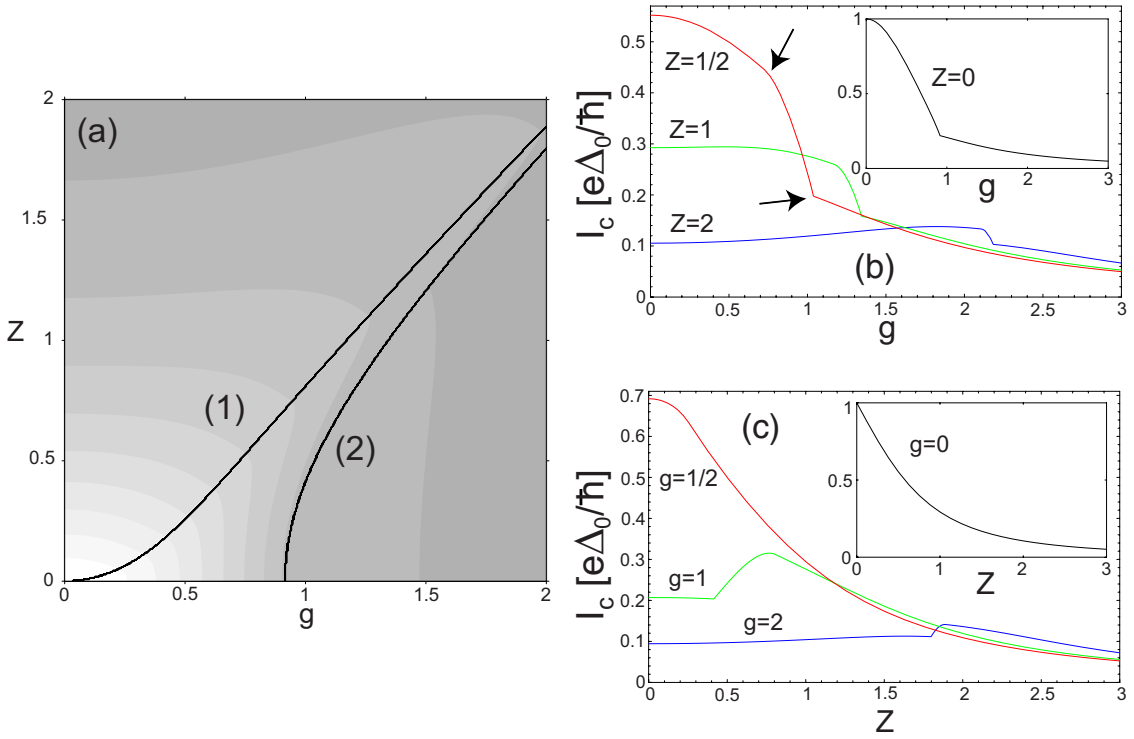

FIG. 3. (Color online) (a) Contour plot of I_c as a function of g and Z [white (black) areas indicate a large (small) critical current]. The solid black lines indicate nonanalyticities in the critical current. (b) I_c as a function of g for several values of Z. (c) I_c as a function of Z for several values of g.

creasing the magnetization of the barrier and thus its magnetic scattering strength. This increase in the magnetization can, for example, be achieved by applying a local magnetic field via atomic force microscopy.[22]

We next consider the temperature dependence of the Josephson current. Here, we find that the splitting of the Andreev states for a nonzero magnetic scattering strength can lead to an unconventional temperature dependence of I_J in which it changes sign with increasing temperature *without* a change in the relative phase, ϕ, between the two superconductors. This temperature dependence is demonstrated in Fig. 5(a), where we assume a BCS temperature dependence of the superconducting gap. In order to understand this sign change, we consider the ϕ dependence of $E_{\alpha,\beta}$ which is shown in Fig. 5(b). At $T=0$, only the branches indicated by 1 and 2, belonging to Andreev states β and α, respectively, are occupied. Since the derivatives $\partial E_\alpha/\partial\phi$ and $\partial E_\beta/\partial\phi$ possess opposite signs, the Josephson currents through them, $I_J^\alpha<0$ and $I_J^\beta>0$, flow in opposite directions with $|I_J^\alpha|>|I_J^\beta|$. Since with increasing temperature, the occupation of branches 2 and 3 changes more rapidly than those of branches 1 and 4, it follows that the magnitude of I_J^β decreases more quickly than that of I_J^α. As a result, the total current, $I_J=I_J^\alpha+I_J^\beta$, eventually changes sign. A possible sign change in I_J with increasing temperature was previously also discussed in Refs. 5 and 6. However, due to the differences between our results for $E_{\alpha,\beta}$ and those in Refs. 5 and 6 (see also Ref. 17) it is presently unclear whether the origin of the sign change in Refs. 5 and 6 is the same as the one discussed here.

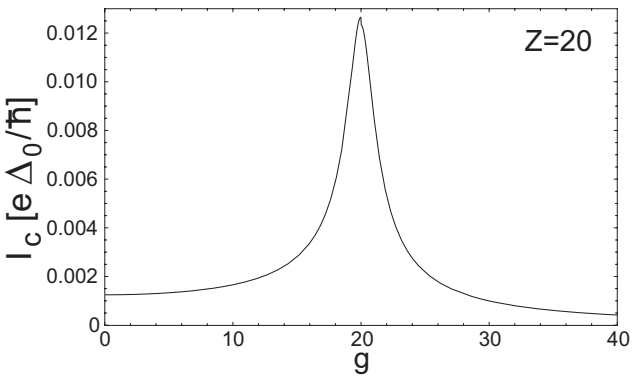

FIG. 4. I_c as a function of g for $Z=20$. The plot of I_c as a function of Z for $g=20$ is virtually indistinguishable from this plot.

The qualitative nature of the temperature dependence can be altered via a change in the couplings g and Z, as follows from Fig. 5(a). We find that in general, a sign change in I_J with increasing temperature occurs when (a) the particlelike components of both Andreev states possess the same spin polarization and (b) ϕ is chosen such that the energy difference between the Andreev states is sufficiently large. These two conditions can easily be satisfied if at least one of the Andreev states exhibits a zero-energy crossing and ϕ is chosen to be close to that crossing in the region where $\langle S_z\rangle=1/2$. A zero-energy crossing, however, occurs only in the gray and black regions of the (g,Z) plane shown in Fig. 2(a). Thus, in order to observe a sign change in I_J with temperature, one should select a barrier whose scattering potentials are close to the $Z=g$ line. Note that a similar temperature-dependent sign change is also predicted to occur in Josephson junctions consisting of triplet superconductors

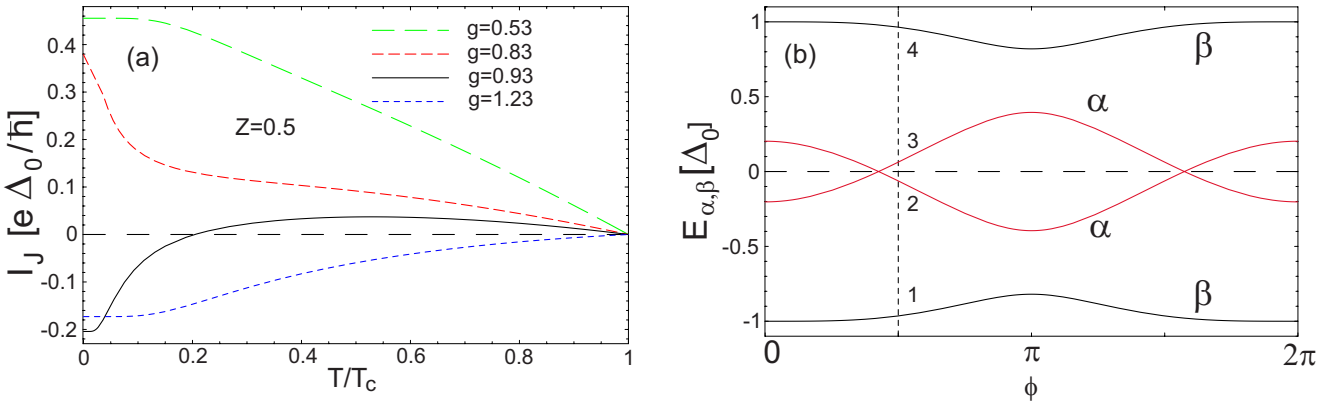

FIG. 5. (Color online) (a) I_J as a function of T/T_c for $\phi=\frac{\pi}{2}$, $Z=1/2$, and several values of g. (b) $\pm E_{\alpha,\beta}$ as a function of ϕ for $Z=1/2$ and $g=0.93$. The dotted line corresponds to the case $\phi=\frac{\pi}{2}$ of (a).

and a ferromagnetic barrier.[23] It is important to stress that the temperature-dependent sign change discussed above is *qualitatively* different from the one reported by Ryazanov *et al.*[4] There, the sign change arises from a transition of the junction from a 0-phase state at high temperatures to a π-phase state at low temperatures due to a temperature-dependent coherence length.[2] In contrast, in our case the sign change arises from a change in the population of the Andreev states, with the relative phase between the superconductors remaining unchanged.

B. Spin transport through Andreev states

We argued in Sec. II B that the origin of the zero total spin current lies in the fact that the spin current through the Andreev states is compensated by a spin current through the continuum states that is equal in magnitude but opposite in sign. The question thus naturally arises if it is possible to separately measure these two contributions to the total spin current. While one could envision several experimental setups in which this could be achieved, for example, by using two Josephson tunneling STM tips, one on each side of the junction, we cannot provide a definite answer to this question at the moment. However, the ability to measure these contributions separately would open exciting venues for using the combined spin and charge degrees of freedom in such a junction. In particular, it would be possible to make use either of a spin polarized (nonzero) charge Josephson current by considering the current through the Andreev states or of a spin Josephson current without a charge Josephson current by considering the current through the continuum states. To exemplify these possibilities, we consider in what follows the spin polarization of the Josephson current through the Andreev states. We first define a spin polarization $\mathcal{P}$ of the Josephson current via

$$\mathcal{P}=\frac{I_{\uparrow}^{\mathrm{AS}}(0)-I_{\downarrow}^{\mathrm{AS}}(0)}{I_{\uparrow}^{\mathrm{AS}}(0)+I_{\downarrow}^{\mathrm{AS}}(0)}=-e\frac{I_{\uparrow}^{\mathrm{AS}}(0)-I_{\downarrow}^{\mathrm{AS}}(0)}{I_J}. \tag{45}$$

For $\mathcal{P}=-1(+1)$, the Josephson current through the Andreev states is completely spin polarized and thus solely carried by spin-$\downarrow$ (spin-$\uparrow$) electrons. In Fig. 6 we present $\mathcal{P}$ as a function of ϕ for $g=1/3$, $Z=2/3$, and $T=0$ [the corresponding charge Josephson current is shown in the second panel of the second row in Fig. 1(b)]. We find that $\mathcal{P}$ is nonzero for all ϕ, and its magnitude reaches a maximum at $\phi=\pi/2$ (note that while $\mathcal{P}\to-1$ at $\phi\to0$, one has at the same time $I_J\to0$). At $T=0$, $I_{\uparrow}^{\mathrm{AS}}$ ($I_{\downarrow}^{\mathrm{AS}}$) is carried solely by the occupied particlelike branch of the β state (α state), as follows immediately from Eq. (32). This is consistent with the observation in Eq. (12) that the particlelike component of the α and β states possess the spin quantum number $S_z=-1/2$ (spin-$\downarrow$) and $S_z=+1/2$ (spin-$\uparrow$), respectively. Since $|I_{0,\alpha}^{v}|>|I_{0,\beta}^{v}|$ for all ϕ, one finds that the Josephson current through the Andreev states is partially spin-$\downarrow$ polarized, as shown in Fig. 6. The degree of spin polarization varies with ϕ due to the changing relative contributions of $I_{0,\alpha}^{v}$ and $I_{0,\beta}^{v}$ to I_J. Finally, for $g=0$, the two Andreev states are degenerate, and hence $\mathcal{P}=0$.

C. First-order quantum phase transition

Another interesting effect arising from the combination of magnetic and nonmagnetic scattering strengths of the barrier is the possibility to tune the Josephson junction through a

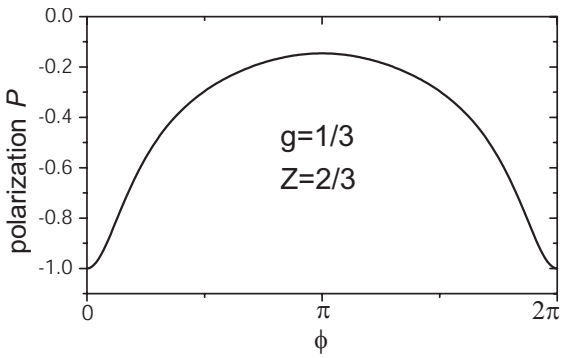

FIG. 6. Spin polarization $\mathcal{P}$ of the Josephson current through the Andreev states at $T=0$ as a function of ϕ for $g=1/3$ and $Z=2/3$.

first-order quantum phase transition in which the ground state of the entire system (i.e., the combined ground state of both superconductors) changes its spin polarization from $\langle S_z\rangle=0$ to $\langle S_z\rangle=1/2$ (assuming without loss of generality that the magnetization of the barrier points along the $\hat{z}$ axis). This type of first-order transition, which is well known from static magnetic impurities in s-wave superconductors, where it was first discussed by Sakurai,[24] can occur either with increasing scattering strength, J, of a magnetic impurity[24] or due to quantum interference effects;[25] its fingerprint is a zero-energy crossing of the impurity-induced fermionic states inside the superconducting gap. The phase transition arises from a level crossing in the superconductor's free energy, $\mathcal{F}$, resulting in a discontinuity of $\partial\mathcal{F}/\partial J$ at the transition, hence the first-order nature of the transition (for a more detailed discussion see Ref. 16). The Josephson junction considered here provides an exciting possibility to tune the system through such a first-order phase transition by varying the phase difference between the superconductors. In Appendix B, we explicitly show that the change in the spin polarization of the junction coincides with the zero-energy crossing of the α state and is thus solely driven by the Andreev states. In contrast, the contribution of the continuum states to the spin polarization vanishes.

As an example of such a phase transition we consider the case $Z=1/3$ and $g=2/3$, for which the energies of the Andreev states and the resulting Josephson current are shown in the third panel in the third row of Figs. 1(a) and 1(b), respectively [we indicate in the panel in Fig. 1(a) the spin quantum number of all the components of the Andreev states]. With increasing ϕ, the α state crosses zero energy at $\phi_c^{\alpha}=2\arccos\sqrt{g^2-Z^2}\approx 0.608\pi$, such that for $\phi>\phi_c^{\alpha}$, the spin-$\uparrow$ component of the α state is particlelike, while its spin-$\downarrow$ component is holelike. This transition results in a change in the ground-state spin polarization from $\langle S_z\rangle=0$ to $\langle S_z\rangle=1/2$. Moreover, the α state crosses zero energy again at $\phi_c^{\alpha'}=2[\pi-\arccos\sqrt{g^2-Z^2}]\approx 1.392\pi$, such that for $\phi>\phi_c^{\alpha'}$ its spin-$\uparrow$ component is holelike, while its spin-$\downarrow$ component is particlelike. As a result, the spin ground state changes from $\langle S_z\rangle=1/2$ back to $\langle S_z\rangle=0$. The range of ϕ for which $\langle S_z\rangle=1/2$ is indicated in the panel of Fig. 1(b) by dotted lines. In general, one finds that $\langle S_z\rangle=1/2$ for those ϕ which satisfy $\cos^2(\phi/2)<g^2-Z^2$. Consequently, as g is further increased (keeping Z fixed), the range of ϕ for which $\langle S_z\rangle=1/2$ increases. When g exceeds the upper critical value $g_c^{>}=\sqrt{1+Z^2}$, one finds $\langle S_z\rangle=1/2$ for all ϕ. In contrast, when g is smaller than the lower critical value $g_c^{<}=Z$, one has $\langle S_z\rangle=0$ for all ϕ. As already mentioned above, the total spin current through the junction is zero even in a state with $\langle S_z\rangle=1/2$.

IV. CONCLUSIONS

In summary, we have studied the Josephson current, I_J, in a 1D Josephson junction consisting of two s-wave superconductors and a thin (δ-function type) ferromagnetic barrier. To this end, we used two complementary theoretical approaches: the BTK method and an approach starting from the quantum-mechanical definition of the current operator. We discussed the general dependence of the charge Josephson current on g and Z, and the relative phase, ϕ, between the two superconductors. Specifically, we showed that in certain regions of the (g,Z) plane, I_J varies continuously with ϕ, while in other regions, and particularly around $Z=g$, I_J exhibits discontinuities. We computed the critical current, I_c, defined as the maximum Josephson current for a given g and Z, and we showed that it possesses two lines of nonanalytic behavior in the (g,Z) plane. These nonanalyticities correspond to discontinuities in the first and second derivatives of I_c (with respect to g or Z). We demonstrated that I_c exhibits qualitatively different dependencies on the scattering strength in different parts of the (g,Z) plane, which opens the interesting possibilities to increase the critical current through the junction by increasing the junction's magnetization. This effect possesses potential applications in the fields of quantum information technology.[26] Moreover, we showed that for certain values of g and Z, the Josephson current changes sign (and thus direction) with increasing temperature without a change in the relative phase between the two superconductors, i.e., without a transition between the 0 and π states of the junction. We showed that this sign change is entirely due to a temperature-dependent change in the occupation of the Andreev states. In agreement with earlier results, we demonstrated that the continuum states do not contribute to the charge current and that therefore, the charge Josephson current is carried entirely by the Andreev states. We also showed that while the total spin Josephson current through the junction is zero, the Andreev states and the continuum states separately carry a nonzero spin current of equal magnitude but opposite sign. The possibility of measuring these contributions separately would open venues for employing the combined spin and charge degrees of freedom in such a junction for potential applications in spin electronics and quantum information technology. Finally, we demonstrate that by changing the phase ϕ between the superconductors, it is possible to tune the junction through a first-order quantum phase transition in which the spin polarization of the superconductor ground state changes between $\langle S_z\rangle=0$ and $\langle S_z\rangle=1/2$.

Experimentally, the effects discussed here could be studied in junctions with magnetically doped insulating barriers based on MgO, ZnO, or TiO_2. In these materials one can imagine varying g independently via the substitution of magnetic dopants such as Co, Mn, etc. and/or by changing their concentration or by applying a small magnetic field, for example, via atomic force microscopy.[22] Moreover, Z can be altered by the choice of material and the junction width. It is possible to control the barrier width of complex oxides using layer-by-layer growth techniques monitored by reflection high-energy electron diffraction (RHEED) on the unit-cell level, which is much smaller than the coherence length of a typical s-wave superconductor. Hence, we expect that the results derived above for a δ-functional barrier should be observable in experimental systems with a nonzero barrier width, d, as long as d is much smaller than the superconducting coherence length. Note that the Josephson behavior

described in this paper will occur in addition to the effects that are expected from the proximity-induced sign change in the superconducting order parameter as a function of the ferromagnetic barrier thickness.[4]

Finally, scattering off the barrier leads to a suppression of the superconducting order parameter near the barrier, which was not accounted for in the approach presented above. However, in *s*-wave superconductors, the length scale over which the order parameter recovers its bulk value near scattering centers (such as a junction) is set by $1/k_F$.[27] This length scale is in general much shorter than both the superconducting coherence length ξ_c and the decay length of the Andreev bound states, κ^{-1}, with $\xi_c \leq \kappa^{-1}$,[12,14] and we thus expect that the inclusion of a spatially varying order parameter does not alter the qualitative nature of our results presented above.

ACKNOWLEDGMENTS

D.K.M. acknowledges financial support from the Alexander von Humboldt Foundation, the National Science Foundation under Grant No. DMR-0513415, and the U.S. Department of Energy under Award No. DE-FG02-05ER46225. B.K. acknowledges financial support from DLR (German Aerospace Center). We would like to acknowledge helpful discussions with P. Fulde, M. Sigrist, M. Kulić, F. Nogueira, I. Eremin, Y. S. Barash, M. Fogelström, P. Brydon, and D. Manske. Moreover, we are grateful to J. Michelsen, V. S. Shumeiko, and G. Wendin for useful communications.

APPENDIX A: CONTRIBUTION OF THE CONTINUUM STATES TO I_J and I_S

For the scattering state wave function of Eq. (4) we make the ansatz

$$\Psi_{n,j}(z) = \sum_{\delta,\epsilon=\pm} \begin{pmatrix} u_{n,j,s,\delta,\epsilon} \\ v_{n,j,s,\delta,\epsilon} \end{pmatrix} e^{i(\delta k_F + \epsilon q)z}, \tag{A1}$$

with $s=L,R$ referring to the left- ($z<0$) and right ($z>0$)-hand sides of the junction, respectively, with $j=\alpha,\beta$, with $q>0$, and where k_F is the Fermi momentum. The corresponding solutions of Eq. (5) are subject to the boundary conditions in Eq. (9). For a given $E_q>|\Delta|$, there are eight continuum states with a positive- and a negative-energy branch for each. For energies that are small compared to the Fermi energy, q is given by Eq. (26).

Define

$$\cosh \gamma = \frac{E_q}{\Delta_0}. \tag{A2}$$

To be specific, consider the negative-energy branches with energy $-E_q$. The BdG equations imply

$$y_{j,s,\delta,\epsilon} \equiv e^{\delta\epsilon\gamma/2} u_{j,s,\delta,\epsilon} = e^{i\phi_s - \delta\epsilon\gamma/2} v_{j,s,\delta,\epsilon}, \tag{A3}$$

with $j=\alpha,\beta$ and $s=L,R$ and where we have omitted the index n labeling the different states of energy $-E_q$.

With $\phi_L=0$ and $\phi_R=-\phi$ and defining

$$e^{i\tau_\pm} \equiv \frac{1+i(Z\pm g)}{\sqrt{1+(Z\pm g)^2}}, \tag{A4}$$

so that

$$-\frac{\pi}{2} < \tau_\pm < \frac{\pi}{2} \tag{A5}$$

and

$$Z = \frac{1}{2}(\tan\tau_+ + \tan\tau_-), \tag{A6a}$$

$$g = \frac{1}{2}(\tan\tau_+ - \tan\tau_-), \tag{A6b}$$

we may organize the boundary conditions [Eq. (9)] in matrix form by writing

$$z_j \equiv M_j y_{j,L} = M_j^* y_{j,R}, \tag{A7}$$

with

$$y_{j,s}^T = (y_{j,s,+,+}, y_{j,s,+,-}, y_{j,s,-,+}, y_{j,s,-,-}) \tag{A8}$$

and

$$M_{\alpha,\beta} = \begin{pmatrix} e^{-\gamma/2} & e^{+\gamma/2} & e^{+\gamma/2} & e^{-\gamma/2} \\ e^{-i\phi/2+\gamma/2} & e^{-i\phi/2-\gamma/2} & e^{-i\phi/2-\gamma/2} & e^{-i\phi/2+\gamma/2} \\ e^{-i\tau_\mp-\gamma/2} & e^{-i\tau_\mp+\gamma/2} & -e^{i\tau_\mp+\gamma/2} & -e^{i\tau_\mp-\gamma/2} \\ e^{-i\tau_\pm-i\phi/2+\gamma/2} & e^{-i\tau_\pm-i\phi/2-\gamma/2} & -e^{i\tau_\pm-i\phi/2-\gamma/2} & -e^{i\tau_\pm-i\phi/2+\gamma/2} \end{pmatrix}, \tag{A9}$$

where the upper (lower) sign corresponds to α (β). Thus the negative-energy scattering states for a given energy $-E_q$ may be represented by y_i. Reinstating labels m and n for the different states for a given energy, we demand that for continuum-normalized orthogonal states $y_{m,j}$ and $y_{n,j}$ hold,

$$\sum_{s=L,R} \sum_{\delta,\epsilon=\pm} y^*_{m,j,s,\delta,\epsilon} y_{n,j,s,\delta,\epsilon} = z^\dagger_{m,j} Q_j z_{n,j} = \delta_{mn} C_r(E_q), \tag{A10}$$

with

$$Q_j \equiv (M_j M_j^\dagger)^{-1} + (M_j M_j^\dagger)^{-1*}, \tag{A11}$$

where $C_r(E_q)$ is real and may be chosen to depend on the energy E_q. That is, finding an orthonormal basis of scattering states for a given energy boils down to diagonalizing the Q_j and using Eqs. (A3) and (A7) to obtain all corresponding coefficients $u_{n,j,s,\delta,\epsilon}$ and $v_{n,j,s,\delta,\epsilon}$. Numerically, we find that

$$\sum_{n(E_q)} (|u_{n,j,s,+,\pm}|^2 - |u_{n,j,s,-,\mp}|^2) = 0, \tag{A12a}$$

$$u^*_{n,j,s,-,+} u_{n,j,s,+,+} - u^*_{n,j,s,-,-} u_{n,j,s,+,-} = 0, \tag{A12b}$$

which are the same for the $v_{n,j,s,\delta,\epsilon}$. Moreover, we numerically obtain

$$\sum_{n(E_q)} [u^*_{n,j,s,+,-} u_{n,j,s,+,+} - u^*_{n,j,s,-,-} u_{n,j,s,-,+}] = d_j A_r(E_q) + i c_s A_i(E_q), \tag{A13}$$

which are the same for the $v_{n,j,s,\delta,\epsilon}$, with $d_{\alpha,\beta} = \pm 1$ and $c_{L,R} = \pm 1$, and where $A_r(E_q)$ and $A_i(E_q)$ are the dimensionless and generally nonzero real coefficient functions.

It is straightforward then to show that

$$\sum_{n(E_q)} \mathrm{Im}(u^*_{n,\alpha} \partial_z u_{n,\alpha} \pm v^*_{n,\alpha} \partial_z v_{n,\alpha} \pm u^*_{n,\beta} \partial_z u_{n,\beta} + v^*_{n,\beta} \partial_z v_{n,\beta}) = \begin{cases} 8kA_i(E_q) \sin 2q|z| \\ 0, \end{cases} \tag{A14}$$

leading immediately to the results in Eq. (27).

APPENDIX B: SPIN GROUND STATE OF THE JUNCTION AND FIRST-ORDER PHASE TRANSITION

The total spin of the system receives contributions from both the Andreev bound states and the scattering states. Define the spin density by

$$\hat{\rho}_S(z) = \frac{\hbar}{2}[\hat{\rho}_\uparrow(z,z') - \hat{\rho}_\downarrow(z,z')]|_{z'=z}, \tag{B1}$$

with $\hat{\rho}_\sigma(z,z')$ from Eq. (15). It is then straightforward to show that

$$\rho_S(z) \equiv \langle \hat{\rho}_S(z) \rangle = \frac{\hbar}{2} \sum_n \left\{ [\rho_{n,u,\alpha}(z) + \rho_{n,v,\alpha}(z)] \tanh \frac{\beta E_{n,\alpha}}{2} - [\rho_{n,v,\beta}(z) + \rho_{n,u,\beta}(z)] \tanh \frac{\beta E_{n,\beta}}{2} \right\}, \tag{B2}$$

where

$$\rho_{n,f,j}(z) \equiv -\frac{1}{2} f^*_{n,j}(z) f_{n,j}(z), \tag{B3}$$

with $f = u, v$ and $j = \alpha, \beta$.

Note that for any given energy, there exist pairs of continuum states that differ only in the spin quantum numbers of their holelike and particlelike branches. This result, combined with the normalization of the continuum states, then yields that their contribution to the spin of the junction vanishes. Using next the normalization of the bound states

$$\int_{-\infty}^{+\infty} dz [u^*_{0,j}(z) u_{0,j}(z) + v^*_{0,j}(z) v_{0,j}(z)] = 1, \tag{B4}$$

with $j = \alpha, \beta$, we obtain that the spin of the system is solely determined by the Andreev bound states and given by

$$\langle S_z \rangle = \int_{-\infty}^{+\infty} dz \rho_S^{\mathrm{AS}}(z) = -\frac{\hbar}{4} \left(\tanh \frac{\beta E_\alpha}{2} - \tanh \frac{\beta E_\beta}{2} \right). \tag{B5}$$

Since our conventions are such that $E_\beta > 0$ always but the sign of E_α can vary, we obtain for $T = 0$,

$$\langle S_z \rangle = \begin{cases} 0 & E_\alpha > 0 \\ \hbar/2 & E_\alpha < 0, \end{cases} \tag{B6}$$

signaling a quantum phase transition caused by the zero-energy crossing of one of the Andreev bound states.

[1] S. A. Wolf, D. D. Awschalom, R. A. Buhrman, J. M. Daughton, S. von Molnar, M. L. Roukes, A. Y. Chtchelkanova, and D. M. Treger, Science **294**, 1488 (2001), and references therein; I. Žutić, J. Fabian, and S. Das Sarma, Rev. Mod. Phys. **76**, 323 (2004).

[2] For recent reviews see S. Kashiwaya and Y. Tanaka, Rep. Prog. Phys. **63**, 1641 (2000); A. A. Golubov, M. Yu. Kupriyanov, and E. Il'ichev, Rev. Mod. Phys. **76**, 411 (2004) and references therein.

[3] L. N. Bulaevskii, V. V. Kuzii, and A. A. Sobyanin, Zh. Eksp. Teor. Fiz. Pis'ma Red. **25**, 314 (1977) [JETP Lett. **25**, 290 (1977)]; A. V. Andreev, A. I. Buzdin, and R. M. Osgood, Phys. Rev. B **43**, 10124 (1991); A. I. Buzdin, B. Vujicic, and M. Yu. Kupriyanov, Zh. Eksp. Teor. Fiz. **101**, 231 (1992) [Sov. Phys. JETP **74**, 124 (1992)].

[4] V. V. Ryazanov, V. A. Oboznov, A. Yu. Rusanov, A. V. Veretennikov, A. A. Golubov, and J. Aarts, Phys. Rev. Lett. **86**, 2427 (2001).

[5] M. Fogelström, Phys. Rev. B **62**, 11812 (2000); M. Andersson, J. C. Cuevas, and M. Fogelström, Physica C **367**, 117 (2002).

[6] Y. S. Barash and I. V. Bobkova, Phys. Rev. B **65**, 144502 (2002).

[7] L. B. Ioffe, V. B. Geshkenbein, M. V. Feigel'man, A. L. Fauchère, and G. Blatter, Nature (London) **398**, 679 (1999).

[8] G. E. Blonder, M. Tinkham, and T. M. Klapwijk, Phys. Rev. B **25**, 4515 (1982).

[9] A. F. Andreev, Sov. Phys. JETP **19**, 1228 (1964).

[10] R. Zikić, L. Dobrosavljević-Grujić, and Z. Radović, Phys. Rev. B **59**, 14644 (1999).

[11] R. A. Riedel and P. F. Bagwell, Phys. Rev. B **57**, 6084 (1998).

[12] A. M. Zagoskin, *Quantum Theory of Many-Body Systems*

(Springer, New York, 1998).
[13] A. Furusaki, Superlattices Microstruct. **25**, 809 (1999).
[14] H.-J. Kwon, K. Sengupta, and V. M. Yakovenko, Eur. Phys. J. B **37**, 349 (2004).
[15] P. G. de Gennes, *Superconductivity of Metals and Alloys* (Addison-Wesley, New York, 1989).
[16] A. V. Balatsky, I. Vekhter, and J.-X. Zhu, Rev. Mod. Phys. **78**, 373 (2006).
[17] In Ref. 5 a splitting of the Andreev states is found to occur for $\phi \neq 0$ only. The reason for this discrepancy with the results discussed above and those in Refs. 6 and 10 lies in the particular form of the S matrix chosen in Ref. 5.
[18] See Sec. 4.5.3 in Ref. 12.
[19] J. Michelsen, V. S. Shumeiko, and G. Wendin, Phys. Rev. B **77**, 184506 (2008).
[20] Note that our Z is, by definition, half the Z of Ref. 14.
[21] Y. Lu, Acta Phys. Sin. **21**, 75 (1965); H. Shiba, Prog. Theor. Phys. **40**, 435 (1968).
[22] P. C. Hammel, Nature (London) **430**, 300 (2004).
[23] B. Kastening, D. K. Morr, D. Manske, and K. Bennemann, Phys. Rev. Lett. **96**, 047009 (2006).
[24] A. Sakurai, Prog. Theor. Phys. **44**, 1472 (1970).
[25] D. K. Morr and N. A. Stavropoulos, Phys. Rev. B **67**, 020502(R) (2003).
[26] B. E. Kane, Nature (London) **393**, 133 (1998).
[27] P. Schlottmann, Phys. Rev. B **13**, 1 (1976); M. I. Salkola, A. V. Balatsky, and J. R. Schrieffer, *ibid.* **55**, 12648 (1997); D. K. Morr and J. Yoon, *ibid.* **73**, 224511 (2006).